# Confined Single-Chain Model of Microphase-Separated Multiblock Copolymers. 2. ABC Copolymers

**Richard J. Spontak***

*Miami Valley Laboratories, Procter & Gamble Company, Cincinnati, Ohio 45239-8707*

**John M. Zielinski**

*Department of Chemical Engineering, The Pennsylvania State University, University Park, Pennsylvania 16802*

*Received May 13, 1991; Revised Manuscript Received August 19, 1991*

ABSTRACT: A three-parameter model based on confined single-chain statistics is developed to address the equilibrium thermodynamics of multicomponent ABC multiblock copolymers in the strong-segregation limit. Here, A and C refer to polystyrene and polyisoprene, respectively, while the chemical nature of the middle (B) block is varied. The utility of ABC copolymers, as described in previous experimental efforts, lies in the fact that the chemically dissimilar blocks are covalently bonded together so that phase intimacy is retained as discrete microdomains form upon microphase separation. Whereas several theoretical formalisms have been proposed for microphase-separated AB diblock and ABA triblock copolymers, no attempts have been made thus far to model systems of the ABC variety. In the present work, predictions are obtained for the free-energy minimum ($\Delta g_{min}$) as a function of both composition ($w_i$) and molecular weight ($M$) and indicate that $\Delta g_{min}$ depends strongly on the chemical characteristics of the B block. Similar behavior is predicted for microstructural parameters such as the interphase volume fractions ($f_{AB}$ and $f_{BC}$), interphase thicknesses ($\lambda_{AB}$ and $\lambda_{BC}$), and microdomain periodicities ($D_{AB}$, $D_{BC}$, and $D$). The effect of compositional asymmetry on both system energetics and microstructural dimensions is also explored, and scaling relationships of the form $M^a$ are identified. The model is further extended to more complex molecular architectures, such as the CACBC pentablock sequence, with good success.

## Introduction

In the first paper[1] of this series on the equilibrium thermodynamics of microphase-separated multiblock copolymers, attention was directed to copolymers of the $(AB)_n$ variety. A model based on the confined single-chain statistics originally developed by Meier[2,3] and Williams et al.[4,5] was used to predict both system energetics and microstructural parameters for two different $(AB)_n$ designs. Those predictions indicated that the molecular configurations of $(AB)_n$ molecules and corresponding morphological characteristics are highly dependent on the number of AB dyads ($n$), as well as on the length of the individual blocks. In this work, the formalism presented earlier for $(AB)_n$ systems is extended to three-block ABC multiblock systems.

Within the past 20 years, significant experimental efforts have been put forth to synthesize neat ABC-block copolymers. Many of these materials consist of polystyrene and a polydiene, usually polybutadiene or polyisoprene. Examples of chemical species used to complete the ABC architecture include poly($\alpha$-methylstyrene),[6] poly(2-vinylpyridine),[7,8] poly(ethylene oxide),[9] poly(4-vinylpyridine),[10,11] poly(ethylene sulfide),[12] and poly[(4-vinylbenzyl)dimethylamine].[13-17] Due to the high degree of control maintained during anionic polymerization,[13-15] ABC copolymers possessing a middle poly[(4-vinylbenzyl)dimethylamine] block have received the most attention in studies aimed at correlating microstructural parameters with molecular characteristics (e.g., composition) and processing conditions (e.g., casting solvents).

The driving force in synthesizing ABC-block copolymers relies on a feature common to all microphase-separated block copolymers: retention of specific homopolymer characteristics in a multiphasic alloy composed of intimately coupled microdomains. Thus, thermodynamically incompatible chemical species, covalently bonded together along the copolymer backbone, remain highly connected (and dispersed) even upon microphase separation. Efforts to increase further (i) the degree of microdomain interconnectivity and (ii) the functional diversity of the blocks have resulted in three- and four-component pentablock copolymers of the CACBC[15,16,18] and CAC′BC[19] varieties, respectively, which are mechanically tougher than their ABC analogues.[16] It should be noted that the morphologies recorded for these pentablock copolymers are very similar to those seen in the ABC materials discussed herein.

Numerous investigations have revealed that ABC materials can exhibit morphologies unlike those normally observed in diblock and triblock copolymers. An example of one of these unique morphologies, discussed in detail by Shibayama et al.[14] and Miyaki et al.,[18] appears as alternating lamellae of two components with dispersed spheres/globules of the third component residing in one of the lamellar microdomains. Another commonly encountered morphology consists of perfectly alternating lamellae (shown in Figure 1) and is similar to that observed in diblock and triblock copolymers. All of these morphologies have been found to be strongly dependent on the composition of the molecule and selectivity of the casting solvent.[14,16,17]

Beside probing morphological features with transmission electron microscopy (TEM) and small-angle X-ray scattering (SAXS), very little has been done to provide a theoretical basis for the established ABC microstructure, in terms of molecular characteristics, in the strong-segregation limit (i.e., the regime where the constituent blocks exhibit strong repulsive interactions). Previous attempts[14] to analyze data obtained from ABC systems in terms of equilibrium thermodynamics have led to the semiempirical application of the diblock models developed by Meier[2,3] and Helfand and Wassermann.[20,21] While the

* To whom correspondence should be addressed.

0024-9297/92/2225-0663$03.00/0 

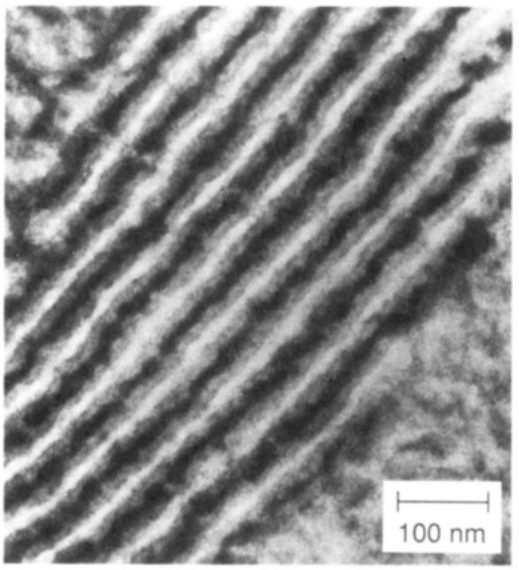


**Figure 1.** Electron micrograph of an ABC block copolymer composed of polystyrene (S), poly[(4-vinylbenzyl)dimethylamine] (A), and polyisoprene (I) in a ratio of 37/39/24 S/A/I and exhibiting a three-phase alternating lamellar morphology. The copolymer, cast from dioxane, was stained with osmium tetroxide so that the I phase appears dark, the A phase gray, and the S phase white. (Reprinted with permission from: Matsushita, Y.; Yamada, K.; Hattori, T.; Fujimoto, T.; Sawada, Y.; Nagasawa, M.; Matsui, C. *Macromolecules* **1983**, *16*, 10. Copyright 1983 American Chemical Society.)

resulting comparisons have been in qualitative agreement with experimental observations, assumptions made during the analyses invoke a hypothetical two-stage microphase-separation scheme.

In the present work, the formalism developed for $(AB)_n$ copolymers is extended to microphase-separated ABC systems possessing the alternating lamellar morphology. The two-parameter confined-chain model originally introduced by Meier[2,3] and Williams et al.[4,5] is replaced here by a three-parameter version to account for the simultaneous free-energy minimization of all unrelated regions in microdomain space. The effects of molecular weight and composition, as well as compositional asymmetry, on system energetics and key microstructural dimensions (illustrated in Figure 2) are investigated and useful scaling relationships identified. Discrete predictions are also provided for microstructural characteristics in more complex systems, such as the three-component CACBC pentablock architecture.

## Thermodynamic Theory

As pointed out earlier,[1] the first step in generating a model based on confined single-chain statistics is to assume that a condensed polymer system can be approximated by a single ideal chain. The validity of this assumption has already been addressed.[22] The second step is to postulate a specific morphology, since the chain statistics are morphology-dependent. All subsequent discussion is therefore limited to the alternating ABC lamellar morphology, which is pictured schematically in Figure 2. In order to simplify the mathematical notation, the ABC designation is often referred to in subsequent discussion as 123.

Since a copolymer system presumably seeks a state of equilibrium upon microphase separation, the difference in molar Gibbs free energy ($\Delta g$) between the microphase-separated state and its homogeneous analogue (of equal molecular composition, weight, and architecture) must be

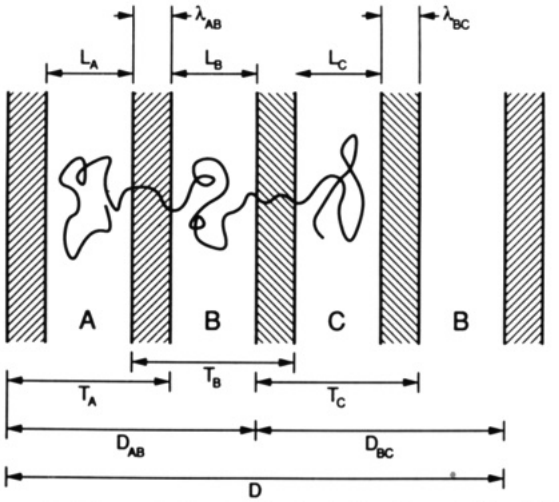


**Figure 2.** Schematic illustration depicting the postulated three-phase lamellar morphology employed in the present model for ABC copolymers. Three distinct microphases ($T_A$, $T_B$, and $T_C$), along with two unrelated interphase regions ($\lambda_{AB}$ and $\lambda_{BC}$), arise from microphase separation. Since each block of the copolymer molecule is chemically dissimilar, no blocks are expected to "loop" in the equilibrium molecular configuration.

minimized with respect to each region of the postulated morphology:

$$\partial \Delta g / \partial A_i = 0 \qquad i = 1, 2, 3, ..., m \tag{1}$$

where $A_i$ is a measure of the $i$th microdomain region and $m$ is the number of such regions that must be considered in the minimization. For an ABC copolymer, $m = 5$ since there are three distinct block cores ($L_i$, where $i$ = A, B, or C, in Figure 2) and two unrelated interphase regions ($\lambda_{AB}$ and $\lambda_{BC}$). Note that $\lambda_{AB} = \lambda_{BA}$ and $\lambda_{BC} = \lambda_{CB}$. The minimized $\Delta g$ function is given by

$$\Delta g_{min} = (\Delta h - T\Delta s)_{min} \tag{2}$$

where $\Delta h$ is the molar enthalpy, $\Delta s$ is the molar entropy, and $T$ is the value of the absolute temperature (298 K). In this work, only conditions yielding negative values of $\Delta g_{min}$ for monodisperse systems will be considered, since these conditions properly correspond to a microphase-separated morphology in the strong-segregation limit. Microstructural dimensions are subsequently deduced implicitly from both $\Delta h$ and $\Delta s$ in eq 2 or explicitly from the values of $A_i$ in eq 1.

The enthalpy can be written as

$$\Delta h = \Delta h^{(1)} + \Delta h^{(2)} \tag{3}$$

where $\Delta h^{(1)}$ accounts for the heat of demixing and $\Delta h^{(2)}$ for the residually mixed interphase regions. If the Flory[23] equation is invoked to calculate the heat of demixing in multicomponent polymeric blends and if the Flory–Huggins $\chi_{ij}$ parameter is replaced by its solubility-parameter analogue, $\Delta h^{(1)}$ is obtained directly from

$$\Delta h^{(1)} = -v \sum_{i<j} \phi_i \phi_j \Delta \delta_{ij}^{\ 2} \tag{4}$$

where $v$ is the total molar volume, $\phi_i$ is the volume fraction of block $i$, and $\Delta\delta_{ij}^{\ 2} = (\delta_i - \delta_j)^2$ is the square of the difference in solubility parameters between microphases $i$ and $j$. Note that $v$ approaches the molecular weight ($M$) of the system as the mass density of each block ($\rho_i$) approaches unity. Since there are only three components in the system, eq

4 can be expanded to read

$$\Delta h^{(1)} = -v(\phi_A\phi_B\Delta\delta_{AB}^2 + \phi_A\phi_C\Delta\delta_{AC}^2 + \phi_B\phi_C\Delta\delta_{BC}^2) \quad (5)$$

where the implicit numerical subscripts 1, 2, and 3 have been replaced by A, B, and C, respectively.

Similarly, $\Delta h^{(2)}$ is written as

$$\Delta h^{(2)} = v\sum_{i=1}^{n-1} f_{ij}\langle\phi_i'\phi_j'\rangle\Delta\delta_{ij}^2 \qquad j = i+1 \quad (6)$$

Here, $f_{ij}$ accounts for the volume fraction of material remaining mixed upon microphase separation and is determined from $\lambda_{ij}/L_{mol}$, where $\lambda_{ij}$ and $L_{mol}$ are the interphase thickness and molecular length, respectively. The interfacial volume-fraction product ($\langle\phi_i'\phi_j'\rangle$) is obtained from

$$\langle\phi_i'\phi_j'\rangle = \int_0^1\left[\phi_i'(x^*)\,\phi_j'(x^*) + \tau_{ij}\left(\frac{d\phi_i'(x^*)}{dx^*}\right)^2\right]dx^* \quad (7)$$

where $x^*$ is the dimensionless distance across the interphase and $\tau_{ij}$ is a normalized long-range interaction parameter equal to $t^2/6\lambda_{ij}^2$ (where $t$ is the Debye length equal to approximately 0.6 nm).[2] As before,[1,5,24] the interphase composition profile of species $i$, $\phi_i'(x^*)$, is approximated by

$$\phi_i'(x^*) = \langle\phi_i\rangle(0)\cos^2(\pi x^*/2) + \langle\phi_i\rangle(1)\sin^2(\pi x^*/2) \quad (8)$$

[Experimental evidence suggests that the interphase composition profile is asymmetric. However, for the sake of continuity in this series and without introducing significant error, only this symmetric profile is considered here.] If the interphase-boundary amplitudes $\langle\phi_i\rangle(0)$ and $\langle\phi_i\rangle(1)$ correspond to pure microphase cores, then $\langle\phi_i\rangle(0) = 1$ and $\langle\phi_i\rangle(1) = 0$. Substitution of eq 8 into eq 7 and retention of the purity conditions yield the following relationship:

$$\langle\phi_i'\phi_j'\rangle = \frac{1+\pi^2\tau_{ij}}{8} \quad (9)$$

Unlike the case of the $(AB)_n$ multiblock copolymer, neither $f_{ij}$ nor $\langle\phi_i'\phi_j'\rangle$ is invariant with regard to the two interphase regions traversed by the ABC molecule (i.e., $f_{AB} \neq f_{BC}$ and $\langle\phi_A'\phi_B'\rangle \neq \langle\phi_B'\phi_C'\rangle$). Thus, it is necessary to retain the individual contributions from each interphase. With these restrictions in mind, eq 9 is substituted into eq 6, which is subsequently expanded to obtain

$$\Delta h^{(2)} = \frac{v}{8}[f_{AB}(1+\pi^2\tau_{AB})\Delta\delta_{AB}^2 + f_{BC}(1+\pi^2\tau_{BC})\Delta\delta_{BC}^2] \quad (10)$$

where $\tau_{AB}$ and $\tau_{BC}$ are normalized with respect to $\lambda_{AB}$ and $\lambda_{BC}$, respectively. Combination of eqs 5 and 10 provides the functional expression for $\Delta h$:

$$\Delta h = -v\left\{\left[\phi_A\phi_B - \frac{f_{AB}}{8}(1+\pi^2\tau_{AB})\right]\Delta\delta_{AB}^2 + \left[\phi_B\phi_C - \frac{f_{BC}}{8}(1+\pi^2\tau_{BC})\right]\Delta\delta_{BC}^2 + \phi_A\phi_C\Delta\delta_{AC}^2\right\} \quad (11)$$

It should be noted here that if A = C and $\phi_A = \phi_C$, $\Delta\delta_{AC} = 0$ and eq 11 corresponds to an equivalent expression for a symmetric ABA triblock copolymer. Furthermore, if A = B or B = C, eq 11 correctly reduces to the expression for a diblock copolymer.

The entropic function ($\Delta s$) is also separated into two parts, one pertaining to confinement of block $i$ to a specific region in microdomain space ($\Delta s_i$) and the other to restriction of the block junction between blocks $i$ and $j$ to the $ij$ interphase region ($\Delta s_{ij}$). Thus,

$$\Delta s = \sum_{i=1}^{3}\Delta s_i + \sum_{i=1}^{2}\Delta s_{ij} \qquad j = i+1 \quad (12)$$

The first term ($\Delta s_i$) is further divided into two contributions. The first ($\Delta s_i^{(1)}$) takes into account the entropy change corresponding to perturbation of the random configuration of block $i$ when the block is confined to $T_i$ (see Figure 2). The second ($\Delta s_i^{(2)}$) reflects the probability of finding block $i$ in $T_i$. Expressions for $\Delta s_i^{(1)}$ have been developed[4,5] from elasticity theory and depend on the block configuration. For instance, if block $i$ is bound at only one end, $\Delta s_i^{(1)}$ is given by

$$\Delta s_i^{(1)} = -{}^3/_2R(\alpha_i^2 - 1 - \ln\alpha_i^2) \quad (13)$$

This expression is valid for the A and C end blocks. However, since the middle B block is anchored at both ends, eq 13 must be rewritten as

$$\Delta s_B^{(1)} = -{}^3/_2R(\alpha_B^2 - 1) \quad (14)$$

In both eqs 13 and 14, $\alpha_i$ is the expansion coefficient of the $i$th block and is defined as

$$\alpha_i \equiv \frac{\langle r_i^2\rangle^{1/2}}{\langle r_i^2\rangle_0^{1/2}} \quad (15)$$

Here, $\langle r_i^2\rangle_0^{1/2}$ and $\langle r_i^2\rangle^{1/2}$ are the respective unperturbed and perturbed root-mean-square (rms) end-to-end distances of the $i$th block. Random-flight chain statistics are employed to obtain values of $\langle r_i^2\rangle_0$:

$$\langle r_i^2\rangle_0 = K_i^2 w_i M \quad (16)$$

where $K_i$ is the Kuhn segment length and $w_i$ is the weight fraction of the $i$th block.

The microdomain region $T_i$ is directly related to $\langle r_i^2\rangle^{1/2}$ through the approach to uniform core density. With confined-chain models of this genre, not all of microdomain space can be uniformly filled. However, as Meier[2,3] points out, this deviation can be minimized, which results in a functional relationship of the form $T_i = (C\langle r_i^2\rangle)^{1/2}$. The constant $C$ has been found to be equal to 2.0 in the case of a block with one free end or 1.5 if both ends of the block are constrained. Thus, in the case of an ABC block copolymer, the following relationships are employed:

$$T_i = (2.0\langle r_i^2\rangle)^{1/2} \qquad i = \text{A or C} \quad (17a)$$

$$T_B = (1.5\langle r_B^2\rangle)^{1/2} \quad (17b)$$

The second contribution to $\Delta s_i$ reflects the probability of finding the $i$th block in $T_i$ and is given by

$$\Delta s_i^{(2)} = R\ln P_i \quad (18)$$

where $R$ is the gas constant and $P_i$ is the corresponding probability function. Expressions for $P_i$ have been derived from solution of the diffusion equation in the case of an infinite parallel-plate geometry and in the absence of an external potential.[2-5] An abbreviated, but accurate,[5] form of $P_i$ for a block with one free end is

$$P_i \approx \frac{4}{\pi}e^{-\zeta_1}\sin\zeta_2 \quad (19a)$$

where $\zeta_1 = \pi^2\langle r_i^2\rangle/6T_i^2$, $\zeta_2 = \pi\beta_{ij}/2$, and $\beta_{ij} = \lambda_{ij}/T_i$. If both ends of a block are constrained to different interphase regions, eq 19a is modified to account for the second

Table I
Characteristics of the Blocks Used in the Calculations of ABC Copolymers Presented Here[a]

| | component A | component B | component C |
|---|---|---|---|
| $\rho$/(g/cm$^3$) | 1.052 | 1.012 | 0.925 |
| $K$/nm | 0.067 | 0.068 | 0.068 |
| $\delta$/H | 9.1 | variable | 8.1 |

[a] Nomenclature defined in text.

boundary condition and becomes

$$P_i \approx \frac{2}{\pi} e^{-\zeta_1} (\sin \zeta_2) \left[ 1 + \cos \left( \frac{\pi (T_i - \lambda_{jk})}{T_i} \right) \right] \quad (19b)$$

Note that, while $\zeta_2$ continues to be a function of $\lambda_{ij}$, the factor reflecting confinement of the second junction to the next interphase is a function of $\lambda_{jk}$ (where $j = i + 1$ and $k = j + 1$). For the middle B block of an ABC copolymer, $\lambda_{ij} = \lambda_{AB}$ and $\lambda_{jk} = \lambda_{BC}$.

The expression for $\Delta s_{ij}$ is similar in principle to eq 18, where the probability of locating a block junction in an interphase is replaced by the fraction of material in the interphase (i.e., $f_{ij}$):

$$\Delta s_{ij} = R \ln f_{ij} \quad (20)$$

It should be remembered that, since $f_{AB} \neq f_{BC}$, $\Delta s_{AB} \neq \Delta s_{BC}$.

With the enthalpic and entropic terms now fully specified, $\Delta g$ is minimized for any given set of molecular characteristics ($w_i$ and $M$) with respect to the five distinct microdomain regions mentioned earlier. However, the number of minimization variables is reduced further by employing a relationship developed by Meier,[2] namely,

$$\alpha_j^2 = \alpha_i^2 \xi_{ij} (w_j / w_i) \quad (21)$$

where $\xi_{ij} = (\rho_i K_i / \rho_j K_j)$. This expression, based on the conservation of block junctions within an interphase region and recently validated[25] for diblock copolymers possessing the lamellar morphology, indicates that both $T_B$ and $T_C$ are related to $T_A$, thereby reducing the number of independent variables to three ($T_A$, $\lambda_{AB}$, and $\lambda_{BC}$). Since $\lambda_{AB}$ is not an explicit function of $\lambda_{BC}$, no further simplifications can be made. Following the methodology put forth by Meier[2,3] and Williams et al.,[4,5] the microstructural dimensions used in the minimization process are made dimensionless through the following definitions:

$$\beta_{AB} \equiv \lambda_{AB} / T_A \quad (22a)$$

$$\beta_{BC} \equiv \lambda_{BC} / T_C \quad (22b)$$

$$\Gamma \equiv T_A^2 / \langle r_A^2 \rangle_0 \quad (22c)$$

The equations used in the free-energy minimization, along with explicit relationships between molecular characteristics and model parameters, are provided in Appendix I. Except for some of the details in the entropic terms, the formalism presented here for an ABC copolymer is also applicable to more complex three-component molecular architectures, such as the CACBC pentablock design.

## Results and Discussion

Homopolymer characteristics (e.g., mass densities and Kuhn constants) for the styrene and isoprene end blocks are provided in Table I. However, molecular parameters for the middle block are not so well-defined. Due to this limitation, $K_B$ is assumed to be approximately equal to $K_A$ and $K_C$ (0.068 nm) and $\rho_B$ is set equal to the density of poly[(4-vinylbenzyl)dimethylamine] (1.012 g/cm$^3$). In light of the variety of candidates for the middle block, these assumptions seem reasonable. Since the value of $\delta_B$ chosen is anticipated to play a key role in the enthalpic contributions and, subsequently, in resulting microstructural predictions, $\delta_B$ is allowed to vary in three increments of $0.5|\Delta\delta_{AC}|$, one within and two outside the interval $[\delta_A, \delta_C]$. That is, since $\delta_A = 9.1$ H and $\delta_C = 8.1$ H, $\delta_B$ is assigned the discrete values of 9.6, 8.6, and 7.6 H. This scheme is believed to provide the most information regarding the relationship between the chemical nature of the middle block and microphase-separated microstructure.

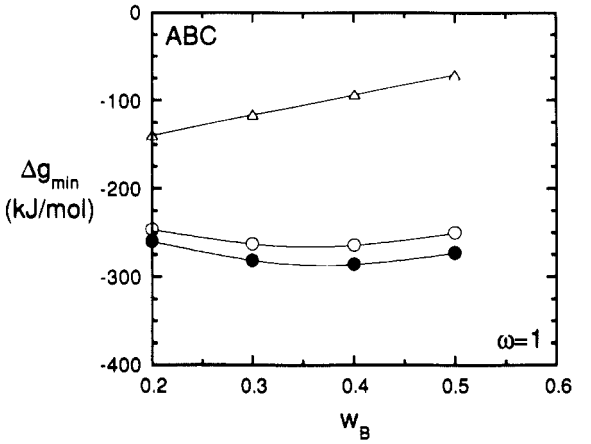


**Figure 3.** Functional relationship of $\Delta g_{min}(w_B, \delta_B)$ evaluated at $M = 200\,000$ for three different values of $\delta_B$: 9.6 H (○), 8.6 H (△), and 7.6 H (●). It is clear that, for symmetric molecules ($\omega = 1$), $\Delta g_{min}(\delta_B = 9.6) \approx \Delta g_{min}(\delta_B = 7.6)$, with both exhibiting a shallow global minimum at $w_B \approx 0.35$. This is not true for $\Delta g_{min}(\delta_B = 8.6)$, which becomes more positive as $w_B$ increases, indicating that the driving force for microphase separation is reduced. The curves shown here, as well as in subsequent figures (unless otherwise specified), are obtained with a cubic-spline algorithm.

**I. Effect of Molar Composition.** The first molecular variable to be addressed here is the composition, expressed in terms of weight fractions of each block. To facilitate discussion, the total molecular weight ($M$) is held constant at 200 000 throughout this section. Since the composition now consists of three variables ($w_A$, $w_B$, and $w_C$), with two degrees of freedom, it is convenient to define $\omega$ as $w_A/w_C$. In the first part of this section, the hypothetical ABC molecules are symmetric (i.e., $w_A = w_C$ or $\omega = 1$). In the second part, the effect of compositional asymmetry is explored when $w_B$ is held constant and $\omega$ is permitted to vary. Since the model presented here is restricted to the alternating lamellar morphology, all $w_i$ are bound between 0.2 and 0.5.

**A. Symmetric ABC Molecules.** Predictions for $\Delta g_{min}$ as a function of $w_B$ ($\omega = 1$) are presented in Figure 3. All of the predictions shown here are negative, indicating that microphase separation is thermodynamically preferred for these particular systems, and are safely removed from the weak-interaction limit ($\Delta g_{min} \approx 0$). The $\Delta g_{min}(w_B)$ trends corresponding to $\delta_B$ greater than $\delta_A$ and less than $\delta_C$ are very similar in appearance and exhibit a shallow minimum at $w_B \approx 0.35$. This behavior suggests that the most energetically favored state is one in which all three blocks are of approximately equal length. It is of interest to note that predictions[1] for microphase-separated $(AB)_n$ copolymers reveal a similar global free-energy minimum when the A- and B-block lengths are approximately equal. This behavior is also predicted[26] for AB diblock copolymers exhibiting lamellar morphology in the weak-interaction limit. When $\delta_A > \delta_B > \delta_C$, the functional behavior of $\Delta g_{min}(w_B)$ in Figure 3 indicates that microphase separation

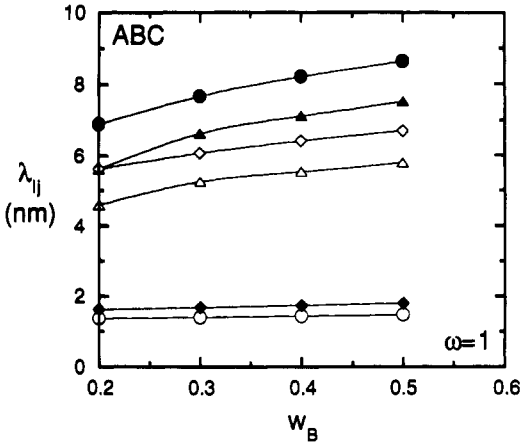


**Figure 4.** Predictions for the interphase thicknesses $\lambda_{AB}$ (open symbols) and $\lambda_{BC}$ (filled symbols) for the three values of $\delta_B$ explored in Figure 3: 9.6 H (○), 8.6 H (△) and 7.6 H (◇). Enlarged interphases due to preferential solubilization of one end block or cosolubilization of both end blocks by the middle (B) block increase with $w_B$, whereas the narrow interphases between the B block and the $i$th end block (where $|\Delta\delta_{Bi}| > 1.0$ H) are almost independent of $w_B$.

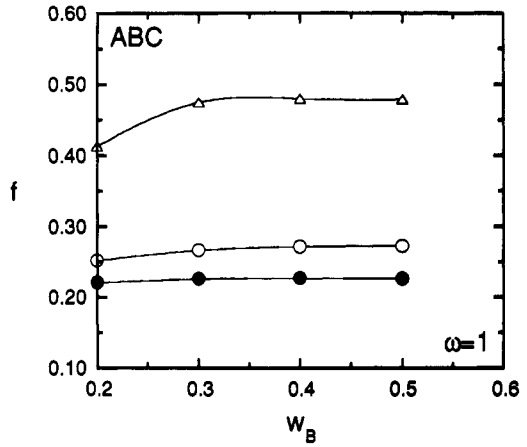


**Figure 5.** Predicted overall interphase volume fraction ($f = f_{AB} + f_{BC}$) of residually mixed (homogeneous) material as a function of $\delta_B$ and $w_B$ for symmetric ABC copolymers. This fraction is almost independent of $w_B$ when $\delta_B$ is outside the $[\delta_A,\delta_C]$ interval but is seen to increase substantially when $\delta_A > \delta_B > \delta_C$. The three symbols in figures such as this one are the same as those in Figure 3.

becomes less favored as $w_B$ increases. This seemingly anomalous trend is due to an increase in the solubilization of both end blocks and is discussed further below.

Figures 4 and 5 show the effect of middle-block composition on the interphase parameters $\lambda_{ij}$ and $f$. Note that $f$ is the sum of all $f_{ij}$, reflecting the total volume fraction of residually mixed (homogeneous) material in the system, and is obtained from

$$f = f_{AB} + f_{BC} = 2(\lambda_{AB} + \lambda_{BC})/D \qquad (23)$$

where $D$ is the microdomain long period (see Figure 2), equal to $L_A + 2L_B + L_C + 2(\lambda_{AB} + \lambda_{BC})$. Several observations from the predicted $\lambda_{ij}(\delta_B,w_B)$ trends warrant discussion. It is clear from Figure 4 that the thickness of interphase $\lambda_{ij}$ depends on the chemical dissimilarity between blocks $i$ and $j$. For instance, the interphase between the blocks possessing the smaller $|\Delta\delta|$ is significantly larger than the one between the blocks with the greater $|\Delta\delta|$. The larger interphase also appears to be much more sensitive to variation in $w_B$, whereas the narrower interphase is almost independent of $w_B$. If $\delta_B$ lies between $\delta_A$ and $\delta_C$, both $\lambda_{AB}$ and $\lambda_{BC}$ are relatively large and are

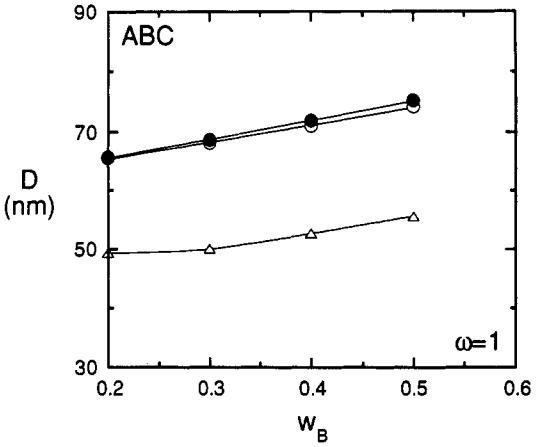


**Figure 6.** Predictions for the microdomain long period ($D$), which is illustrated in Figure 2. Predicted $D(\delta_B,w_B)$ are observed to increase with $w_B$ for all three values of $\delta_B$. However, $D(\delta_B=8.6)$ is noticeably less than $D(\delta_B=9.6)$ or $D(\delta_B=7.6)$, whereas $D(\delta_B=9.6) \approx D(\delta_B=7.6)$. This decrease in $D$ as $\delta_A > \delta_B > \delta_C$ is attributed to the increased fraction of homogeneous material induced by cosolubilization of both end blocks by the middle block.

dependent on $w_B$. Another interesting feature of Figure 4 is that there appears to be a symmetry about the solubility parameter differences. That is, $\lambda_{AB}(\delta_B=9.6) \approx \lambda_{BC}(\delta_B=7.6)$ and $\lambda_{BC}(\delta_B=9.6) \approx \lambda_{AB}(\delta_B=7.6)$. This apparent symmetry is found throughout many of the predictions presented here.

Further discussion of the interphase thicknesses presented in this work warrants a comparison with predictions from mean-field theory.[20,21] As pointed out in the first paper of this series,[1] the interphase employed here extends over the entire length of the composition profile, whereas the linearized interphase ($\lambda'$) defined in mean-field theory corresponds to the span of the slope evaluated at the midpoint composition of the profile. This difference in definition results in $\lambda'$ being considerably smaller (by 36%) than $\lambda$.[5] This means that the narrow $\lambda$ seen in the lower part of Figure 4 measure approximately 0.9–1.0 nm in terms of $\lambda'$, and the thicker interphases (the result of preferential and mutual end-block solubilization) range in $\lambda'$ from 2.9 to 5.7 nm, depending on composition.

The mean-field theory developed by Helfand and associates[20,21] utilizes the narrow interphase approximation (NIA)—i.e., the asymptotic condition at infinite block lengths—denoted here as $\lambda_\infty'$. In the case of the narrow interphases seen in Figure 4, $\lambda_\infty' \approx 1.0$ nm, while end-block solubilization results in an interphase measuring approximately 3.0 nm. Thus, it is clear from these comparisons that the narrow-interphase predictions obtained with the present formalism are certainly in good agreement with those obtained from mean-field theory, whereas considerable differences arise between the two theories in the case of enlarged interphases.

Predictions for $f(\delta_B,w_B)$ in Figure 5 reveal that the fraction of interphase material in ABC copolymers does *not* depend very much on composition when $\delta_B$ is *outside* the $[\delta_A,\delta_C]$ interval. This predicted behavior is in agreement with that obtained[27] for microphase-separated diblock copolymers with $\Delta\delta_{AB} \approx 0.8$ H. However, due to the size of the enlarged interphases, $f$ is found to increase significantly (by a factor of about 2 at $M$ = 200 000) if $\delta_A > \delta_B > \delta_C$.

The long period $D$ is presented as a function of $\delta_B$ and $w_B$ in Figure 6. For all three values of $\delta_B$, $D$ is seen to increase slightly with $w_B$, especially when $\delta_B$ is outside the $[\delta_A,\delta_C]$ interval. Again note that $D(\delta_B=9.6) \approx D(\delta_B=7.6)$. An interesting feature observed in Figure 6 is that the

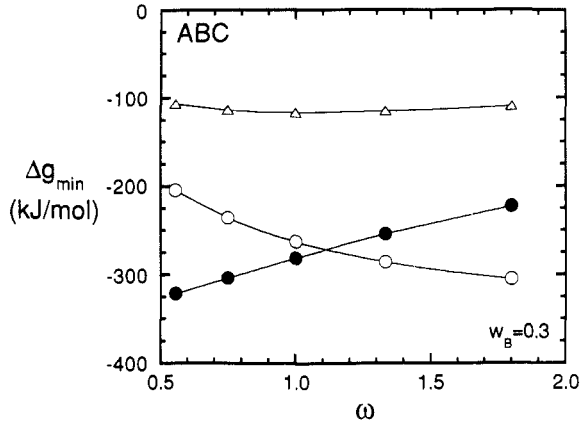


**Figure 7.** Effect of compositional asymmetry on predicted $\Delta g_{min}(\omega,\delta_B)$ where $\omega = w_A/w_C$. In this and the following two figures, $w_B$ is held constant at 0.3. Here, $\Delta g_{min}(\delta_B=8.6)$ is not very sensitive to $\omega$, whereas both $\Delta g_{min}(\delta_B=9.6)$ and $\Delta g_{min}(\delta_B=7.6)$ become more positive as the length of the block which is preferentially solubilized by the middle block increases. Use of the block physical parameters tabulated in Table I results in the observed crossover point at $\omega \approx 1.1$.

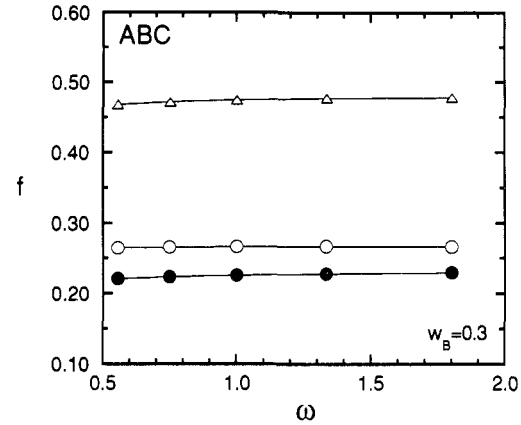


**Figure 8.** Plot of $f$ vs $\omega$. As with most of the predicted microstructural parameters, $f(\omega,\delta_B)$ shows very little dependence on $\omega$. This behavior suggests that, for any given $M$, microstructural dimensions are relatively independent of block length. However, the effect of $\delta_B$ on $f$ is as pronounced as first seen in Figure 5.

predicted $D$ for the case of $\delta_A > \delta_B > \delta_C$ is noticeably less than the one obtained when $\delta_B$ is outside $[\delta_A,\delta_C]$. This feature is presumably attributable to the considerable residually mixed fraction of material that results when $\delta_B$ is between $\delta_A$ and $\delta_C$ (see Figure 5).

The accuracy of these predictions can be determined by a comparison with experimental data; however, microstructural data of this type are not common. Shibayama et al.[14] have used TEM and SAXS to determine $D$ for an ABC copolymer possessing a molecular weight of 164 000 and a composition of 37 wt % styrene, 39 wt % (4-vinylbenzyl)dimethylamine, and 24 wt % isoprene. The magnitude of $D$, they discovered, was found to depend on the selectivity of the casting solvent employed. Films cast from benzene, a relatively neutral solvent, possessed an apparent equilibrium morphology with $D \approx 57$ nm. The predicted $D$ for this ABC system, assuming $\delta_B \approx 9.3$ H (based on the group-contribution methods of van Krevelen[28]), is 53.4 nm. The agreement between predicted and measured $D$ is reasonably good.

**B. Asymmetric ABC Molecules.** In the last section, predictions have been presented for the case when $\omega = 1$ and $w_B$ varies. In this section, the effect of compositional asymmetry is explored by setting $w_B$ equal to an arbitrary composition (0.3) and allowing $\omega$ to vary. Since all $w_i$ are bound between 0.2 and 0.5 (for retention of the postulated alternating lamellar morphology, $\omega$ is correspondingly limited to the range between 0.5 and 2.0.

In Figure 7, $\Delta g_{min}(\delta_B,\omega)$ is observed to exhibit two different types of behavior, depending on $\delta_B$. In the cases when $\delta_B$ is outside $[\delta_A,\delta_C]$, $\Delta g_{min}$ becomes more negative as the length of the end block $i$ most closely related to the middle block ($j$) is reduced. This trend is due to the fact that as the $i$th end block decreases in length, the other ($k$) end block becomes longer, thereby increasing the extent of thermodynamic incompatibility between the $j$ and $k$ blocks. It is interesting to note that the $\Delta g_{min}(\delta_B=9.6,\omega)$ and $\Delta g_{min}(\delta_B=7.6,\omega)$ curves cross at $\omega \approx 1.1$. If the physical characteristics (i.e., $\rho$ and $K$) of the A and C blocks were identical, the crossover point would be at $\omega = 1.0$. These relationships, in conjunction with those in Figure 3, can consequently be considered as the free-energy part of a sensitivity analysis designed to optimize the lengths of each block. Figure 7 also reveals one other noteworthy feature: the functionality of $\Delta g_{min}(\delta_B=8.6,\omega)$. In this case, the ratio of the A-block length to the C-block length has little effect on $\Delta g_{min}$, within a reasonable range of $\omega$. This apparent anomaly is investigated elsewhere.[29]

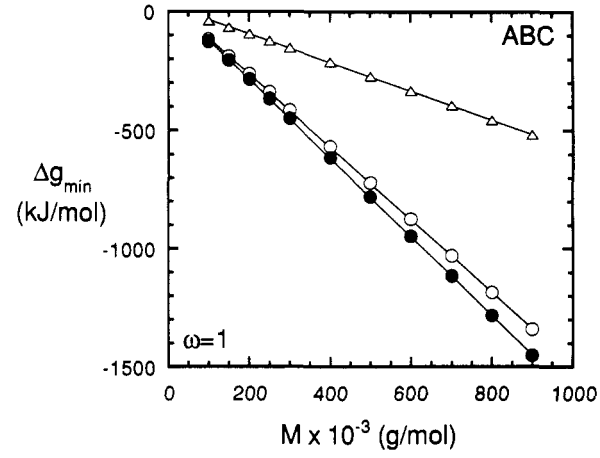


**Figure 9.** Predicted $\Delta g_{min}(M,\delta_B)$ for symmetric ABC molecules ($\omega = 1$) and $w_B = 0.4$. Both the magnitude of $\Delta g_{min}$ and its slope ($\partial \Delta g_{min}/\partial M$) are very dependent on the value of $\delta_B$ chosen. The apparent linearity of each $\Delta g_{min}(M)$ is attributed to the linear dependence of the enthalpy on the molar volume ($\approx M$). The curves are least-squares regressions of the predictions.

Predictions for the interphase volume fraction ($f$) as functions of $\delta_B$ and $\omega$ are shown in Figure 8. As in Figure 5, the value of $\delta_B$ has the most dramatic effect on $f$. Here, however, $f$ is observed to be almost completely independent of $\omega$ over the entire range of $\omega$ studied. While the effect of $\delta_B$ remains pronounced, similar behavior is also predicted for $\lambda_{ij}(\delta_B,\omega)$ and $D(\delta_B,\omega)$ and indicates that these microstructural parameters do not vary considerably with composition in a molecule of constant $M$. For this reason, these predictions are not provided here.

**II. Effect of Molecular Weight.** The predictions provided in the previous two sections indicate that the hypothetical copolymer system of most interest, in terms of system energetics, microstructural dimensions, and molecular conformation, possesses $w_A \approx w_B \approx w_C$. With $\omega = 1$ and $w_B = 0.4$, the effect of molecular weight on these parameters is explored in this section. Since the weak-interaction limit must be avoided for these predictions to be valid, the lower limit of the molecular weight range employed here is 100 000, whereas the upper limit is arbitrarily set to 900 000.

In Figure 9, $\Delta g_{min}$ is presented as functions of both $\delta_B$ and $M$. The apparent linearity in the predicted relation-

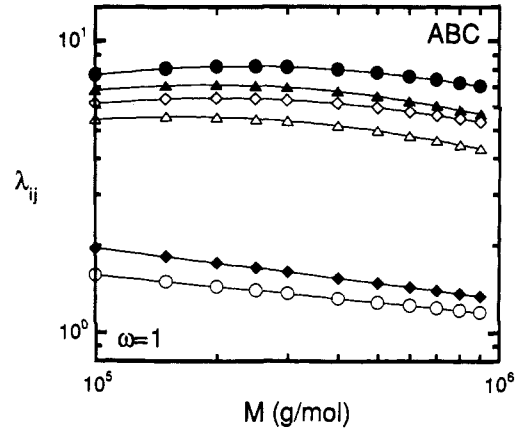


**Figure 10.** Interphase thicknesses $\lambda_{AB}$ and $\lambda_{BC}$ presented as functions of both $M$ and $\delta_B$. It is clear from this figure that neither interphase is strongly dependent on $M$, decreasing by no more than 1.0 nm over the $M$ range shown. Enlarged interphase regions from both preferentially solubilized and cosolubilized end blocks do not scale with $M$, whereas the narrow interphases (lower part of figure) scale as $M^a$, where $a$ lies between −0.14 and −0.18. Some of the curves are obtained from a least-squares regression of predicted values, and the symbols are the same as those used in Figure 4.

ships is due to the influence of $v$ ($\approx M$) in the enthalpic contribution (eq 11). Both $\Delta g_{min}(\delta_B=9.6,M)$ and $\Delta g_{min}(\delta_B=7.6,M)$ exhibit similar behavior of comparable magnitude over the entire $M$ range. However, the magnitude of $\Delta g_{min}(\delta_B=8.6,M)$ and its slope ($\partial \Delta g_{min}/\partial M$) are predicted to be significantly less negative than those corresponding to the other two $\Delta g_{min}$ functions. This trend is due to the fact that the middle block tends to cosolubilize both end blocks to a similar degree if $\delta_A > \delta_B > \delta_C$, whereas one end block is preferentially solubilized to a greater extent when $\delta_B$ is outside $[\delta_A,\delta_C]$. If $\delta_B$ is increased further outside this interval (i.e., $\delta_B < 7.6$ H or $\delta_B > 9.6$ H), $\partial \Delta g_{min}/\partial M$ becomes increasingly more negative.

Consider now the case in which the opposite occurs, $\delta_B$ approaches either $\delta_A$ or $\delta_C$. For any given set of molecular characteristics, there exists a critical solubility parameter difference, $|\Delta\delta_{ij}|_c$, or equivalently a critical $\chi_{ij}$ parameter, that must be maintained for valid use of models in the strong-segregation limit. If $|\Delta\delta_{ij}| < |\Delta\delta_{ij}|_c$, then local density fluctuations are no longer negligible, and a model based on the weak-interaction limit, like those of Leibler[26] or McMullen and Freed,[30] must be utilized. One interesting feature of this hypothetical condition is that the cosolubilized end and middle blocks can enter the weak-segregation limit, while the other block pair remains in the strong-segregation limit! When $\delta_B$ degenerates to being equal to $\delta_A$ or $\delta_C$, then the model collapses to the corresponding diblock analogue. However, when $\delta_B$ lies between $\delta_A$ and $\delta_C$, the functional relationship of $\Delta g_{min}(M)$ becomes very sensitive to $\Delta\delta_{AB}$ and $\Delta\delta_{BC}$, a point which will be discussed further elsewhere.[29]

The predicted effects of increasing $M$ on the microstructural parameters describing the interphase regions are illustrated in Figures 10 and 11. In Figure 10, the interphase thicknesses ($\lambda_{AB}$ and $\lambda_{BC}$) are shown for the three values of $\delta_B$ used throughout this work. The trends seen earlier (Figure 4) are again apparent, but this figure also demonstrates that the functional relationship $\lambda_{ij}(M)$ is strongly dependent on $\delta_B$. For those enlarged interphases resulting from the proximity of $\delta_B$ to either $\delta_A$ or $\delta_C$ or both (upper part of Figure 10), the effect of increasing $M$ is not apparent until $M > 400\,000$. Even at higher values of $M$, the nonlinear decrease in $\lambda_{ij}$ is almost negligible (ca. <1.0 nm). The narrow interphase regions (lower part

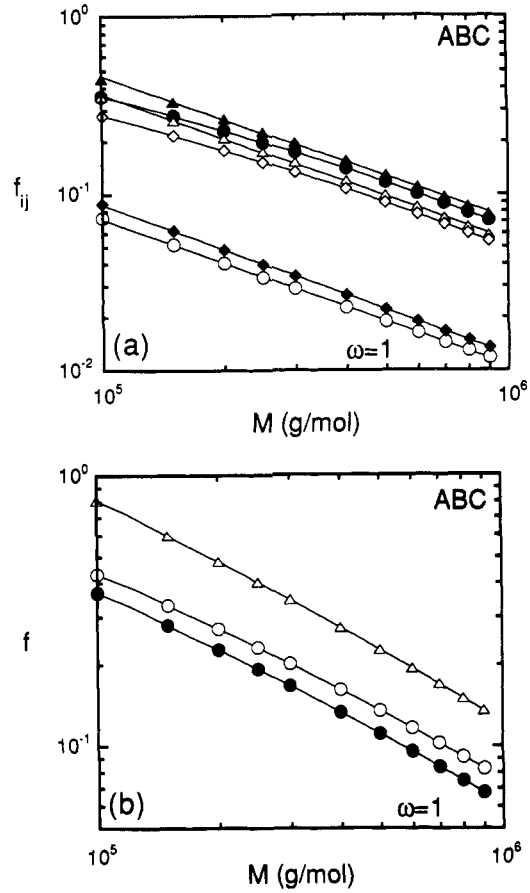


**Figure 11.** Predicted functional relationships for (a) $f_{AB}(M,\delta_B)$ and $f_{BC}(M,\delta_B)$ and (b) $f(M,\delta_B)$. Both $f_{ij}$ and $f$ are found to decrease systematically with $M$. In (a), $f_{ij}$ corresponding to interphases that have been enlarged due to preferential solubilization by the middle block do not scale with $M$, while the narrow and cosolubilized interphases do, with the scaling exponent ($b$) varying from −0.81 to −0.86. In (b), $f$ ($=\sum_i f_{ij}$, $j = i + 1$) is observed not to scale with $M$. Curves illustrating an $M^b$ dependence are obtained with a least-squares regression of the predicted $f_{ij}$.

of Figure 10) appear to scale as $M^a$, where the exponent $a$ lies between −0.14 and −0.18. (Recall that these $\lambda$ can be easily converted[5] to linearized $\lambda'$ by multiplying them by 0.64.) All of these predicted trends suggest that neither $\lambda_{AB}$ nor $\lambda_{BC}$ is a strong function of $M$ for the values of $\delta_B$ employed here.

In Figure 11, the functions $f_{ij}(\delta_B,M)$ and $f(\delta_B,M)$ are shown. Note that the $f_{ij}$ in Figure 11a reflect the individual interphase thicknesses provided in Figure 10. It is apparent from Figure 11a that some $f_{ij}$ scale as $M^b$, while others do not. Those that do possess this relationship are the ones corresponding to (i) narrow interphases between the middle B and $i$th end blocks (where $|\Delta\delta_{Bi}| > 1.0$ H, in the present work) and (ii) enlarged interphases resulting from $\delta_A > \delta_B > \delta_C$. The $f_{ij}$ that do not scale as $M^b$ refer to the enlarged interphases resulting from partial and preferential solubilization of the B block with one of the end blocks. Values of the scaling exponent ($b$) are determined from a least-squares algorithm to lie between −0.81 and −0.86, in agreement with that discerned earlier for microphase-separated diblock copolymers.[1,31] The total volume fraction of homogeneous material ($f = \sum_i f_{ij}$, $j = i + 1$) is presented as a function of $M$ in Figure 11b. The predicted relationships are in line with those seen in Figure 11a; however, none of these $f(\delta_B,M)$ appear to scale directly with $M$.

Predictions for the long spacings ($D$) of these ABC copolymers with $\omega = 1$ and $w_B = 0.4$ are presented in Figure

**Table II**
**Molecular Characteristics of and Model Predictions for Some of the CACBC[a] Copolymers in Reference 18**

| molecular weights/$10^4$ | | | | | | exptl param | predicted param[b] | | | | |
|---|---|---|---|---|---|---|---|---|---|---|---|
| $M_C^{(1)}$ | $M_A$ | $M_C^{(2)}$ | $M_B$ | $M_C^{(3)}$ | $\langle M_C \rangle^c$ | $D'$ [d]/nm | $\Delta g_{min}$/(kJ/mol) | $\lambda_{AB}$/nm | $\lambda_{BC}$/nm | $f$ | $D'$/nm |
| 6.6 | 9.8 | 6.5 | 9.7 | 6.6 | 6.6 | 51 | -444.6 | 2.8 | 1.8 | 0.09 | 48.5 |
| 3.5 | 9.1 | 3.5 | 8.9 | 3.2 | 3.4 | | -277.7 | 2.8 | 1.8 | 0.13 | 35.1 |
| 6.0 | 8.9 | 6.0 | 12.9 | 5.7 | 5.9 | 44 | -458.6 | 2.7 | 1.8 | 0.09 | 43.8 |

[a] C = isoprene, A = styrene, and B = (4-vinylbenzyl)dimethylamine. [b] The solubility parameter of the B block is estimated to be approximately 9.3 H, on the basis of the group contribution method by van Krevelen.[28] [c] $\langle M_C \rangle = [\sum_i M_C^{(i)}]/3$. [d] $D'$ is the repeat distance from one C block to another, estimated from the electron micrographs provided in Figures 7 and 8 of ref 18.

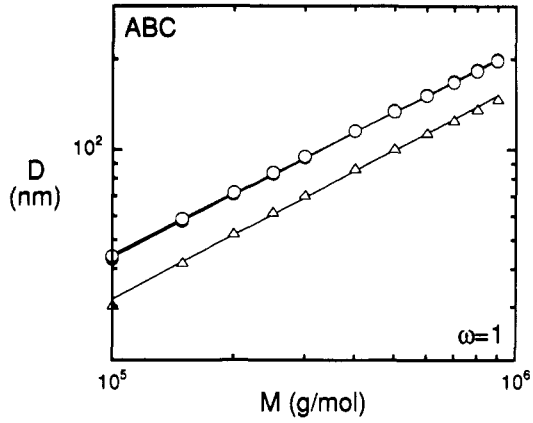


**Figure 12.** Predictions for the microdomain long spacing ($D$) as a function of $M$ and $\delta_B$. It is clear from this figure that values of $D(\delta_B=9.6)$ are almost identical to those of $D(\delta_B=7.6)$ over the entire range of $M$ shown. These two functions are also observed to scale as $D \sim M^c$, where $c \approx 0.68$ as derived from a least-squares regression of the predicted $D$. This scaling behavior is very similar to that obtained from AB diblock copolymers and indicates non-Gaussian chain stretching along the lamellar normal. The $D(\delta_B=8.6)$ relationship exhibits curvature, but a corresponding value of $c$ is approximated as 0.68.

12. The $D(\delta_B=9.6,M)$ and $D(\delta_B=7.6,M)$ functions in Figure 12 are almost identical, scaling as $M^c$, whereas $D(\delta_B=8.6,M)$ possesses slight curvature. The average value of $c$ is 0.68, in quantitative agreement with previous work on microphase-separated AB diblock copolymers,[3,5,21,24,32,33] and indicative of chain stretching along the lamellar normal. Sdranis and Kosmas[34] have recently addressed the issue of block and molecular expansion in ABC block copolymers on theoretical grounds and have shown that the non-Gaussian behavior of the molecule is strongly dependent on the chemical interactions of the blocks. The short spacings ($D_{AB}$ and $D_{BC}$ in Figure 2) sum to $D$ and consequently exhibit similar scaling behavior as in Figure 12 and are not provided here for that reason.

**III. Effect of Molecular Architecture.** In all of the previous sections, only the ABC architecture has been addressed. In principle, though, the formalism presented here is applicable to any multiblock architecture, providing that (i) the equilibrium morphology consists of alternating lamellae and (ii) the blocks are sufficiently long to employ assumptions valid only in the strong-segregation limit. Efforts to synthesize more exotic multicomponent linear block copolymers have resulted in both three-component CACBC[15,16,18] and four-component CAC'BC[19] materials. As observed with TEM, these copolymers can also exhibit a microphase-separated lamellar morphology, identical to the one illustrated in Figure 2 for ABC designs. While it would be possible to ascertain the functional relationships of the system energetics and microstructural dimensions for CACBC and CAC'BC materials, the number of variables needed to be considered is far too numerous to have such relationships included here. Rather, we simply point out the utility of the present approach by predicting the microstructural characteristics of three of the copolymers described in detail in ref 18. These three materials all exhibit alternating lamellae and possess C blocks (isoprene) of nearly equal length (see Table II). To facilitate matters, the average length of the three C blocks is utilized in subsequent calculations.

Predictions corresponding to the three CACBC copolymers are tabulated in Table II. Only predicted microdomain periodicities can be compared with experimental data, since the short period ($D'$) can be estimated from the $OsO_4$-stained isoprene lamellae in electron micrographs. Note that $D'$ is equivalent to the $D_{ij}$ mentioned earlier. It is clear that the predicted $D'$ are in good agreement with experimental results. The predictions in Table II indicate that these multicomponent copolymers can be modeled with confined-chain statistics in the strong-segregation regime ($\Delta g_{min} < 0$) and that the resulting microstructural dimensions ($\lambda_{ij}$ and $D'$) are certainly reasonable.

## Conclusions

A three-parameter thermodynamic model based on the confined single-chain statistics originally developed by Meier[2,3] and Williams et al.[4,5] is proposed for multicomponent ABC multiblock copolymers. This family of materials offers great potential for specific applications, such as mosaic membranes,[19] due to the functionality of each block. Predictions have been presented here to elucidate three different effects on system energetics and microstructural dimensions: (i) composition and compositional asymmetry, (ii) molecular weight, and (iii) molecular architecture. In all of these cases, the chemical nature (i.e., solubility parameter) of the middle block has been allowed to vary. Resultant predictions clearly indicate that the three-phase lamellar morphology established by an ABC copolymer is most noticeably affected if the solubility parameter of the middle block lies between those of both end blocks. Compositional studies suggest that, based on the minimum free-energy function, the most energetically stable ABC copolymer exhibiting alternating lamellae should possess approximately equal block lengths. Many of the microstructural dimensions have been found to be very weak functions of composition in a copolymer of constant molecular weight. However, several of these dimensions, whose analogues are known to scale with molecular weight in microphase-separated AB and ABA block copolymers, have been shown to retain this scaling behavior in ABC copolymers, indicating that the molecules are stretched along the lamellar normal. The formalism presented here is also applicable to more complex multicomponent molecular architectures.

**Acknowledgment.** We express sincere gratitude to the Pennsylvania State University for computing time. One of us (J.M.Z.) would also like to thank the Exxon Chemical Co. for a fellowship.

## Appendix I. Relationships between Molecular Characteristics and Model Parameters

The enthalpic ($\Delta h$) and entropic ($\Delta s$) contributions to the free-energy function ($\Delta g$) have been provided by individual terms in the text, reflecting the fact that the minimization results presented here were obtained using such numerical methods as the golden and gradient search protocols. These expressions can also be combined and written in terms of the minimization parameters $\beta_{AB}$, $\beta_{BC}$, and $\Gamma$. For instance, $\Delta h$ can be recast from eq 11 to read

$$\Delta h = -M\left(\frac{w_A}{\rho_A}+\frac{w_B}{\rho_B}+\frac{w_C}{\rho_C}\right)\left\{\left[\phi_A\phi_B-\frac{\beta_{AB}T_A}{4D}-\frac{\pi^2t^2}{24D\beta_{AB}T_A}\right]\Delta\delta_{AB}{}^2+\left[\phi_B\phi_C-\frac{\beta_{BC}T_C}{4D}-\frac{\pi^2t^2}{24D\beta_{BC}T_C}\right]\Delta\delta_{BC}{}^2+\phi_A\phi_C\Delta\delta_{AC}{}^2\right\} \quad \text{(A1)}$$

where

$$D = (1-2\beta_{AB})T_A + (1-2\beta_{BC})T_C + 2T_B \quad \text{(A2)}$$

and, by eqs 15–17 and 21–22,

$$T_A = K_A(\Gamma w_A M)^{1/2} \quad \text{(A3a)}$$

$$T_B = \frac{K_B w_B}{2}\left(\frac{3\xi_{AB}\Gamma M}{w_A}\right)^{1/2} \quad \text{(A3b)}$$

$$T_C = K_C w_C\left(\frac{\xi_{AC}\Gamma M}{w_A}\right)^{1/2} \quad \text{(A3c)}$$

Note that, since $L_{mol} = D/2$ in the case of ABC copolymers, $f_{ij} = \lambda_{ij}/L_{mol} = 2\lambda_{ij}/D$.

The complete entropic term accounting for deformation of the blocks ($\Delta s^{(1)}$) is given by

$$\Delta s^{(1)} = -\frac{3R}{2}\left[\frac{\Gamma}{2}\left(1+\xi_{AB}\frac{w_B}{w_A}+\xi_{AC}\frac{w_C}{w_A}\right)-3-2\ln\left(\frac{\Gamma}{2}\right)-\ln\left(\xi_{AC}\frac{w_C}{w_A}\right)\right] \quad \text{(A4)}$$

Likewise, combining the expressions which describe block confinement in microdomain space ($\Delta s^{(2)}$) and simplifying yield

$$\Delta s^{(2)} = R\left\{\ln(2\mu_{AB})+\ln(2\mu_{BC})-\frac{\pi^2}{6}+\left[\ln\mu_{AB}-\frac{\pi^2}{9}\right]\left[1-\cos\left(\frac{\pi\beta_{BC}T_C}{T_B}\right)\right]\right\} \quad \text{(A5)}$$

where

$$\mu_{ij} \equiv \frac{2}{\pi}\sin\left(\frac{\pi\beta_{ij}}{2}\right) \quad \text{(A6)}$$

The loss of entropy associated with the restriction of the block junctions to their respective interphase regions ($\Delta s^{(3)} = \Delta s_{AB} + \Delta s_{BC}$) has been provided in terms of $f_{ij}$ in eq 20, which, in light of the relationships presented here, can be rewritten as

$$\Delta s^{(3)} = R\ln\left(\frac{4\beta_{AB}\beta_{BC}T_AT_C}{D^2}\right) \quad \text{(A7)}$$

It follows immediately from eq 2 that the free-energy function to be minimized with respect to $\beta_{AB}$, $\beta_{BC}$, and $\Gamma$ is consequently given by

$$\Delta g = \Delta h - T(\Delta s^{(1)} + \Delta s^{(2)} + \Delta s^{(3)}) \quad \text{(A8)}$$

## References and Notes


(1) Zielinski, J. M.; Spontak, R. J. *Macromolecules*, preceding paper in this issue.
(2) Meier, D. J. In *Block and Graft Copolymers*; Burke, J. J., Weiss, V., Eds.; Syracuse University Press: Syracuse, NY, 1973; Chapter 6. Meier, D. J. *J. Polym. Sci., Part C* **1969**, *26*, 81; *ACS Polym. Prepr.* **1974**, *15*, 171.
(3) Meier, D. J. In *Thermoplastic Elastomers: A Comprehensive Review*; Legge, N. R., Holden, G., Schroeder, H. E., Eds.; Hanser Publishers: New York, 1987; Chapter 12.
(4) Leary, D. F.; Williams, M. C. *J. Polym. Sci., Polym. Phys. Ed.* **1973**, *11*, 345; **1974**, *12*, 265.
(5) Henderson, C. P.; Williams, M. C. *J. Polym. Sci., Polym. Phys. Ed.* **1985**, *23*, 1001; *Polymer*, **1985**, *26*, 2021; **1985**, *26*, 2026.
(6) Fielding-Russell, G. S.; Pillai, P. S. *Polymer* **1974**, *15*, 97.
(7) Price, C.; Lally, T. P.; Stubbersfield, R. *Polymer* **1974**, *15*, 541.
(8) Fielding-Russell, G. S.; Pillai, P. S. *Polymer* **1977**, *18*, 859.
(9) Koetsier, D. W.; Bantjes, A.; Feijen, J. *J. Polym. Sci., Polym. Chem. Ed.* **1978**, *16*, 511.
(10) Arai, K.; Kotaka, T.; Kitano, Y.; Yoshimura, K. *Macromolecules* **1980**, *13*, 1670.
(11) Kudose, I.; Kotaka, T. *Macromolecules* **1984**, *17*, 2325.
(12) Cooper, W.; Hale, P. T.; Walker, J. S. *Polymer* **1974**, *15*, 175.
(13) Matsushita, Y.; Choshi, H.; Fujimoto, T.; Nagasawa, M. *Macromolecules* **1980**, *13*, 1053.
(14) Shibayama, M.; Hasegawa, H.; Hashimoto, T.; Kawai, H. *Macromolecules* **1982**, *15*, 274.
(15) Funabashi, H.; Miyamoto, Y.; Isono, Y.; Fujimoto, T.; Matsushita, Y.; Nagasawa, M. *Macromolecules* **1983**, *16*, 1.
(16) Isono, Y.; Tanisugi, H.; Endo, K.; Fujimoto, T.; Hasegawa, H.; Hashimoto, T.; Kawai, H. *Macromolecules* **1983**, *16*, 5.
(17) Matsushita, Y.; Yamada, K.; Hattori, T.; Fujimoto, T.; Sawada, Y.; Nagasawa, M.; Matsui, C. *Macromolecules* **1983**, *16*, 10.
(18) Miyaki, Y.; Iwata, M.; Fujita, Y.; Tanisugi, H.; Isono, Y.; Fujimoto, T. *Macromolecules* **1984**, *17*, 1907.
(19) Takahashi, S.-I.; Matsumura, K.; Toda, M.; Fujimoto, T.; Hasegawa, H.; Miyaki, Y. *Polym. J.* **1986**, *18*, 41.
(20) Helfand, E. In *Recent Advances in Polymer Blends, Grafts and Blocks*; Sperling, L. H., Ed.; Plenum Press: New York, 1974. Helfand, E. *Macromolecules* **1975**, *8*, 552. Helfand, E. In *Developments in Block Copolymers*; Goodman, I., Ed.; Applied Science: London, 1982; Vol. I.
(21) Helfand, E.; Wassermann, Z. R. *Macromolecules* **1976**, *9*, 879; **1978**, *11*, 960; **1980**, *13*, 994.
(22) Curro, J. G.; Schweizer, K. S. *Macromolecules* **1987**, *20*, 1928.
(23) Flory, P. J. *Principles of Polymer Chemistry*; Cornell University Press: Ithaca, NY, 1953; p 549.
(24) Spontak, R. J.; Williams, M. C.; Agard, D. A. *Macromolecules* **1988**, *21*, 1377.
(25) Spontak, R. J.; Samseth, J.; Zielinski, J. M. *Polymer*, in press.
(26) Leibler, L. *Macromolecules* **1980**, *13*, 1602.
(27) Spontak, R. J. *Colloid Polym. Sci.* **1989**, *267*, 808.
(28) van Krevelen, D. W. *Properties of Polymers: Their Estimation and Correlation with Chemical Structure*; Elsevier Science: New York, 1976; pp 152–154.
(29) Zielinski, J. M.; Spontak, R. J. *Macromolecules*, submitted for publication.
(30) McMullen, W. E.; Freed, K. F. *J. Chem. Phys.* **1991**, *93*, 9130.
(31) Spontak, R. J.; Williams, M. C. *J. Polym. Sci., Polym. Phys. Ed.* **1990**, *28*, 1379.
(32) Hashimoto, T.; Shibayama, M.; Kawai, H. *Macromolecules* **1980**, *13*, 1237. Hashimoto, T.; Fujimura, M.; Kawai, H. *Macromolecules* **1980**, *13*, 1660.
(33) Matsushita, Y.; Mori, K.; Saguchi, R.; Nakao, Y.; Noda, I.; Nagasawa, M. *Macromolecules* **1990**, *23*, 4313.
(34) Sdranis, Y. S.; Kosmas, M. K. *Macromolecules* **1991**, *24*, 1341.


**Registry No.** S/A/I (block copolymer), 106529-33-3.